AIMS Energy, 4(6): 906-920.
DOI: 10.3934/energy.2016.6.906
Received: 18 August 2016
Accepted: 18 November 2016
Published: 30 November 2016

http://www.aimspress.com/journal/energy

Research article

Design of optimum reference temperature profiles for energy saving control of indoor temperature in a building

Sumera I. Chaudhry and Manohar Das*

Department of Electrical and Computer Engineering, Oakland University, Rochester, MI 48309, USA

*** Correspondence:** Email: das@oakland.edu; Tel: +1-248-370-2237.

Abstract: This paper presents a technique for designing optimum reference temperature profiles for energy-efficient control of indoor air temperature in buildings. Arbitrarily chosen reference temperature profiles are often fraught with undesirable consequences, such as thermal discomfort for a building's occupants or high consumption of fuels and electricity. An optimized reference temperature profile, on the other hand, attempts to seek a desired trade-off between the level of discomfort and amount of energy consumed. Also, the use of such optimized temperature profiles for adaptive control of indoor building temperature is discussed in details and some simulation results are presented.

Keywords: Building temperature control; Energy saving control; optimum temperature profile; adaptive temperature control

1. Introduction

A great deal of research efforts is being spent these days on reducing the cost of heating, ventilation and cooling (HVAC) of residential and commercial buildings, because such costs constitute about 40–50% of the total electrical energy consumed in USA and elsewhere. Such efforts are deemed important, because they may not only result in cost savings but also reduce the carbon footprints of buildings.

The reduction of HVAC energy consumption in buildings often requires deployment of advance control techniques, because the building's characteristics and parameters are often unknown, their occupancy levels vary during different times in a day, and the outdoor conditions also vary widely from day-time to night-time and from season to season. In recent years, the advances in wireless sensors and sensor networks, installation of smart meters in buildings and advent of smart grid technology have

provided an impetus for development of advanced control schemes for reducing the energy consumed for heating/cooling of buildings, while assuring thermal comfort for their occupants.

A variety of advanced HVAC control schemes have appeared in the literature [1-10]. Examples include classical PID controller, PID cum fuzzy logic control (PID-FLC) and PID combined with model predictive control (PID-MPC) [1], optimal, adaptive and intelligent control [2], artificial neural network (ANN) based control, and fuzzy logic (FL) controller [3]. Also, other approaches include model predictive control (MPC) [4-8], and predicted mean vote (PMV) based adaptive or PID controller [9,10]. In general, the performance of plain PID controllers have been found to be poor compared to other advanced control schemes, such as PID-FLC, PID-MPC, and MPC controllers. However, in terms of real-time computational cost, PID turns out to be the simplest, whereas MPC and PID-MPC seem to be most complicated controllers, because they require real-time optimization of certain cost functions.

Among all HVAC control schemes proposed to date, the MPC controllers have been found to be most efficient and effective [5,6]. The MPC scheme introduced in [5] deserves a special mention because it uses a comfort based cost criterion and poses the control problem as a sequential linear programming [LP] problem. This LP formulation of the control problem makes it more attractive than the conventional MPC schemes that attempt to solve a sequential nonlinear optimization problem. The performance of the proposed controller is compared with that of two classical PID controllers and the proposed MPC controller is shown to perform significantly better than the PID controllers and also reduce energy consumption. The MPC controller studied in [6] is a reference temperature tracking controller that optimizes a weighted sum of tracking errors and control efforts. It is an interesting and important study because the controller was implemented in an actual building and shown to be highly effective and energy efficient compared to the existing controller.

None of the above controllers, however, employ fully self-adaptive control techniques in the sense that the controller estimates all the parameters governing the nonlinear thermal dynamical model of a building and use it to design adaptive HVAC controllers. Two such adaptive controllers were presented in [11] and [12]. The adaptive control scheme presented in [11] addresses control of indoor temperature only, whereas the scheme presented in [12] addresses control of both temperature and relative humidity. Also, the control methodology presented in [11] is simpler compared to the one presented in [12]. A comprehensive review of all the control techniques proposed for controlling indoor temperature in buildings can be found in [13].

With the goal of improving a building's energy efficiency, some research efforts have also focused on design of optimum HVAC systems and controllers. For instance, a technique for determining the optimal settings of a heat exchanger outlet water temperature to minimize the total energy consumption of pumps under varying working conditions was presented in [14]. Also, a number of other researchers have focused their efforts on global optimization of overall HVAC systems [15-17].

The goals of a typical energy-efficient HVAC controller are two-fold: (i) reduction of fuel and electricity consumption, and (ii) assurance of adequate comfort for the building's occupants. A majority of the HVAC controllers [1-11] mentioned above attempt to meet these goals by employing control techniques that are designed to track a desired reference temperature profile. More often than not, however, such reference temperature profiles are chosen rather arbitrarily without consideration of their relative merits or demerits. Thus, the resulting controller is not optimized for the right balance between comfort and energy efficiency. We attempt to address this shortcoming in this paper. In essence, we present a technique for designing optimum reference temperature profiles and

demonstrate its usage for energy-efficient control of indoor air temperature in a building. The design of adaptive one-step ahead (OSA) and weighted one-step-ahead (WOSA) controllers, similar to the ones presented in [11], is discussed here. These controllers are basically MPC controllers involving a one-step control horizon, which are very easy to implement, although they are less efficient compared to conventional MPC controllers. These are merely used as demonstration tools here, and in fact, the proposed optimum temperature profile construction strategy can also be useful for other temperature tracking control schemes, such as PID, fuzzy and MPC controllers.

The organization of this paper is as follows. Section 2.1 presents methodology and objectives. A dynamical model of a building's thermal system is summarized in Section 2.2. Section 2.3 describes a technique for designing an optimum indoor temperature profile, which is utilized to design an adaptive indoor temperature controller in Section 2.4. Section 3 presents some simulation results and a discussion. Finally, some concluding remarks are given in Section 4.

2. Method

2.1. An Overview of Methodology and Objectives

The aim of this paper is two-fold. First, it presents a technique for generating an optimum indoor temperature profile that provides a desired trade-off between occupants' comfort and energy efficiency. Second, it demonstrates the usage of the above temperature profile for adaptive control of indoor temperature in a building.

The goal of a smart building temperature control system is to maintain the indoor temperature of a building by achieving an optimum tradeoff between heating/cooling energy consumption and occupants' thermal comfort. The overall heating/cooling energy consumed in a building can be divided into two parts: (i) energy consumed to maintain the steady-state conditions, and (ii) energy consumed to raise (or lower) temperature to a different level. The latter becomes an important part of the overall energy saving strategy, because during favorable outdoor conditions and/or low occupancy levels and at nights, the target temperature can be lowered (during heating season) or raised (during cooling season) to save energy, and subsequently brought back to the desired level whenever desired. A significant amount of energy saving can be realized in the process.

To demonstrate the above energy saving principle, we consider a winter (heating) season and assume prior knowledge of the user's desired temperature levels during peak hours (when people are active and electronics/appliances are on) and off-peak hours (when there is no occupancy or no activity and no electronics are being used). Next, with the dual goal of energy efficiency and occupants' comfort in mind, we formulate a multi-objective cost function that consists of a weighted sum of both costs, with individual weights being chosen by the user. This cost function is then minimized to generate an optimum reference temperature profile that attains the desired temperature levels during different times of the day. Finally, this optimum temperature profile is used to design a one-step ahead adaptive controller, which is similar to the one presented in [11].

2.2. Dynamical Model of a Building's Thermal System

To start with, a dynamical model of a building's thermal system is summarized in this section. However, since heating and cooling dynamics are very similar, we discuss only heating dynamics here for the sake of brevity. Also, with the control design in mind, the complexity of the dynamical model is

kept to a minimum. Thus, although a very detailed multi-input single output transfer function model of a building's thermal system is available in [18], we restrict this study to a simpler model proposed in [9]. Also, we restrict our attention to a model of an air-controlled building, even though the optimization strategy presented in this paper is general in nature and applicable to other types of building models as well.

Following the footsteps of Calvino et al. [9] and IBPT toolbox [19], a simplified dynamical model of an air-controlled building's thermal system (during a heating season) can be described by the following equation:

$$\frac{c_i d\theta_a(t)}{dt} = \dot{m}(t)\eta c_f(\theta_{f_{av}} - \theta_a(t)) + H_T(\theta_{out}(t) - \theta_a(t)) + H_{gains} \quad (1)$$

where $\theta_a(t)$ denotes the indoor temperature at time t, θ_{out}(t) is the outdoor temperature at time t, c_i denotes the total heat capacity of the indoor air mass and other objects inside the building, c_f is the specific heat of the warming carrier (air), $\dot{m}$(t) denotes the flow rate of the warming carrier (air), $\theta_{f_{av}}$ denotes the average air temperature inside the heat exchanger, η is a constant that depends on the heating source and heat transfer efficiency of the heat exchanger. Also, H_T denotes the global heat transfer coefficient of the building envelope and H_{gains} denotes the heat gains from various internal and external sources. A more detailed description of the above terms can be found in references [9] and [19].

At this point, for the sake of notational simplicity, it would be convenient to make the following changes of variables:

$$y = \theta_a,\ u = \dot{m},\ y_{out} = \theta_{out},\ y_{f_{av}} = \theta_{f_{av}}$$

Thus, Equation (1), which represents a simplified dynamical model of the building, now takes the following form:

$$\frac{dy}{dt}(t) = Au(t)(y_{f_{av}} - y(t)) + B(y_{out}(t) - y(t)) + C \quad (2)$$

where *y(t)* denotes the indoor temperature, *u(t)* is the flow rate of the warming carrier and A, B and C denote the model parameters that are given by:

$$A = \frac{c_f \eta}{c_i} \quad (3a)$$

$$B = \frac{H_T}{c_i} \quad (3b)$$

$$C = \frac{H_{gains}}{c_i} \quad (3c)$$

As considered in [1], we assume that the thermal losses due to ventilation are insignificant, but the convective part of all heat sources, such as the solar heat gains and the heat gains from the heating system or casual gains, are considered to be parts of the model equation. The following discrete time model is derived from the system Equation (1) using a first order Euler approximation for $\frac{dy}{dt}$ with a sampling interval, T_s:

$$\frac{y(k+1) - y(k)}{T_s} = Au(k)(y_{f_{av}} - y(k)) + B(y_{out}(k) - y(k)) + C \quad (4)$$

where k denotes the discrete time index (i.e., k = 1,2,3…) and the time instance, kT_s, is simply denoted by k. The above thermal model is characterized by three unknown parameters, namely, A, B and C.

2.3. A Technique for Designing an Optimum Reference Temperature Profile

In this section, we consider the choice of a desired reference temperature profile over a period of 24 hours from 00:00 to 23:59.

2.3.1. General Characteristics of a Reference Temperature Profile

To start with, one can argue that we can choose a temperature profile arbitrarily depending on the heat delivery capacity of our furnace. For instance, if our furnace has a very high heat delivery capacity, we can choose a profile shown in Figure 1a, which shows the desired temperature settings between hours of 00:00 (12 am) to 23:59 (11:59 pm). This profile is characterized by lower temperature settings during low occupancy levels and/or night hours, and also steep ascents from lower temperature levels to higher ones, whenever desired. On the other hand, if our furnace has a relatively low heat delivery capacity, we can choose a profile shown in Figure 1b, which is characterized by relatively slow ascents from lower temperature levels to higher ones, whenever necessary. Unfortunately, both of these profiles represent suboptimal choices, because a steep-ascent profile minimizes thermal discomfort for the occupants at the cost of increased fuel, electricity and capital costs, whereas a slow-ascent profile lowers fuel, electricity and capital expenses at the cost of increased thermal discomfort. This motivates us to look for an optimum reference temperature profile that seeks a desired trade-off between the conflicting goals of low energy cost and low level of thermal discomfort for the occupants. Such a profile should look similar to Figure 1b, but incorporate optimum upswing sections.

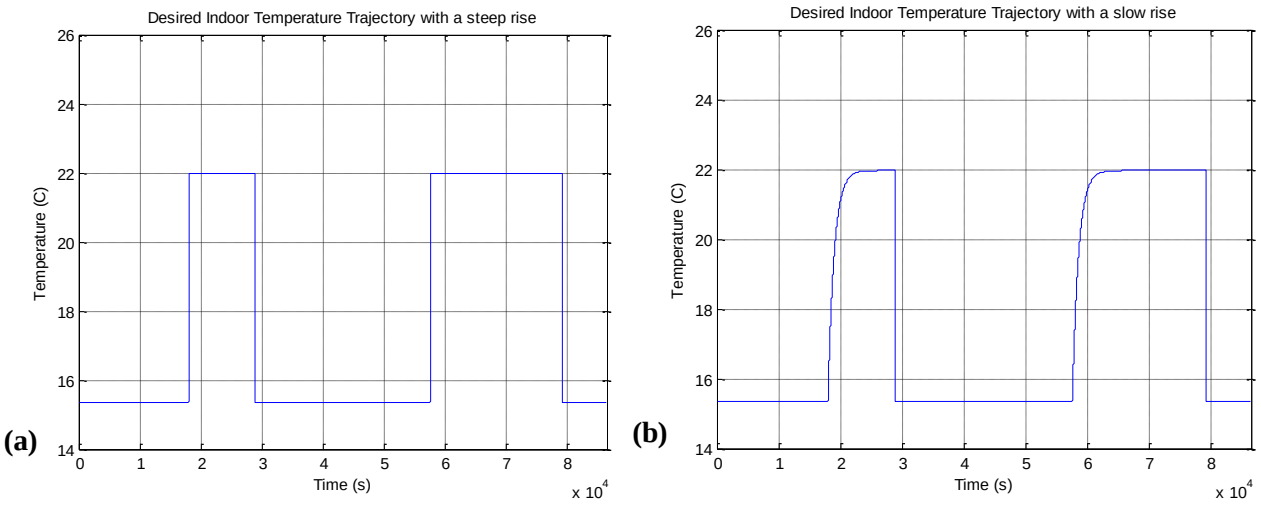

Figure 1. Arbitrarily chosen indoor temperature profiles: (a) Steep-ascent, (b) Slow-ascent between hours of 00:00 (12 am) to 23:59 (11:59 pm).

2.3.2. Design of an Optimum Reference Temperature Profile

In view of above, let us assume that our desired optimum indoor temperature profile has a shape similar to Figure 1b above with upswing sections described by:

$$y = T_c + (T_d - T_c) * (1 - e^{-\alpha t}) \tag{5}$$

where T_c denotes a (current) lower temperature setting (°C) and T_d represents a desired higher temperature (°C). Also, $\frac{1}{\alpha}$ denotes the time constant that controls the rate of rise of temperature from T_c to T_d. A small value of α will give a slow-ascent profile similar to Figure 1b, whereas a relatively large value of α will give a steep-ascent profile similar to Figure 1a.

The task of an optimal reference temperature profile generator involves finding an optimum value of α, which gives a desired trade-off between the conflicting goals of minimizing the heating energy cost, $I_e(\alpha)$, and minimizing the cost of thermal discomfort, $I_c(\alpha)$, for the occupants. This can be formulated as a multiobjective optimization problem as follows.

To start with, we define the cost functions, $I_e(\alpha)$ and $I_c(\alpha)$. First, notice that I_e can be calculated by integrating the thermal power supplied by the heat generating devices, $\dot{q_f}$(t), over a desired time interval:

$$I_e = \int_0^T \dot{q_f}(t)\ dt = c_i \int_0^T (A * u(t) * \left(y_{fav} - y(t)\right))dt \tag{6}$$

Next, we assume that the instantaneous thermal discomfort can be measured as the deviation of the actual level of thermal comfort from the desired one. In order to do this, however, we need a commonly accepted measure of thermal comfort. For the sake of simplicity, we use predicted mean vote (PMV) [20,21] as our measure of thermal comfort. It is defined as an index that predicts the mean value of the votes of a large group of persons on a seven-point thermal sensation scale based on the heat balance of human bodies. In its original form [20], it predicts the thermal sensation as a function of clothing, insulation, activity level, ambient temperature, mean radiant temperature, relative air velocity and relative humidity. The seven point thermal sensation scale ranges from −3 to +3, corresponding to the sensations from cold to hot, respectively, with the zero value indicating a comfortable or neutral sensation (i.e., neither hot nor cold).

Fanger's original PMV equation is a rather complicated nonlinear function of all the above variables [20]:

$$PMV = (0.325e^{-0.042M} + 0.032)[M - 0.35(43 - 0.061M - p_a) - 0.42(M - 50) - 0.0023M(44 - p_a) \\ -0.0014M(34 - T_i) - 3.4 * 10^{-8} f_{cl}((T_{cl} + 273)^4 - (T_{mrt} + 273)^4) - f_{cl} h_c (T_{cl} - T_i)] \tag{7a}$$

where T_{cl}, h_c and p_v are given by:

$$T_{cl} = 35.7 - 0.032M - 0.18I_{cl}[3.4 * 10^{-8} f_{cl}((T_{cl} + 273)^4 - (T_{mrt} + 273)^4) - f_{cl} h_c (T_{cl} - T_i)] \tag{7b}$$

$$h_c = \begin{cases} 2.05(T_{cl} - T_i)^{0.25} & for \quad 2.05(T_{cl} - T_i)^{0.25} > 10.4\sqrt{v} \\ 10.4\sqrt{v} & for \quad 2.05(T_{cl} - T_i)^{0.25} < 10.4\sqrt{v} \end{cases} \tag{7c}$$

$$p_v = p_s RH/100 \tag{7d}$$

In the above equations, T_i denotes the ambient air temperature (°C), T_{mrt} is the mean radiant temperature (°C), M denotes the metabolic rate per unit body surface area (kcal/hr m^2), v is the relative velocity (m/s), p_v denotes the water vapor pressure in ambient air (mmHg), I_{cl} is the thermal resistance of the clothing (unit: 1 clo = 0.18 °C m^2 h/kcal), h_c denotes the convective heat transfer coefficient (kcal/m^2 h °C), f_{cl} is the ratio of the surface area of the clothed body to the surface area of the nude body, T_{cl} is the mean temperature of outer surface of the clothed body (°C), p_s is the saturated water vapor in ambient air (mmHg) and RH is the relative humidity in percent.

Since the above equation is complicated, a simplified equation would be highly desirable for simulation studies. With this in mind and following the lead of Calvino et al. [9], we assume constant values for some of the parameters, namely, M = 1 kcal/hr m^2, I_{cl} = 1 clo, v = 0.15 m/s, RH = 50%. Also, assuming the conditions stated in Appendix C of ASHRAE standard 55 [21] to be valid, we let $T_{mrt} = T_i$. In this case, as explained in [9], PMV becomes a linear function of indoor temperature, T_i or y (in our notation). This approximate relationship between PMV(t) and y(t) is given by [9]:

$$PMV(t) = 0.2262 * y(t) - 4.969 \tag{8}$$

It may be pointed out that although the above relationship is valid only under limited operating conditions, it does not in any way preclude the usage of the original Equations (7a–d) in practical applications.

Assuming PMV is given by (8), the instantaneous thermal discomfort can be measured as the total deviation of the actual PMV from the desired one, which is assumed to be zero. Thus, the cost of discomfort I_c, is given by:

$$I_c(\alpha) = \int_0^T PMV(t)^2 \, dt \tag{9}$$

At this point, it would be helpful to find out how $I_e(\alpha)$ and $I_c(\alpha)$ are affected by the choice of α. From Equation (5), notice that a small value of α gives a slow-ascent profile similar to Figure 1b, whereas a relatively large value of α gives a steep-ascent profile similar to Figure 1a. Thus, with increase of α, the cost of heating energy, $I_e(\alpha)$, will go up, but the cost of discomfort, $I_c(\alpha)$, will go down. As mentioned earlier, the goal of an optimal reference temperature profile generator is to find an optimum value of α, which gives a desired trade-off between the conflicting goals of minimizing both heating energy cost, $I_e(\alpha)$, and the cost of thermal discomfort, $I_c(\alpha)$. This is clearly a multi-objective optimization problem that can be solved using a variety of approaches [22]. In this study, we investigate one of the simplest approaches known as the weighted sum method. Since both $I_e(\alpha)$ and $I_c(\alpha)$ are nonnegative functions of α, we consider minimization of a weighted sum of these two cost functions, i.e., the optimization problem is:

$$Min_\alpha \, f(\alpha, \beta) = \beta * [Ie(\alpha)] + (1 - \beta) * [Ic(\alpha)] \tag{10}$$

where $0 \leq \beta \leq 1$ dictates the weights associated with I_e and I_c, respectively. Any efficient single variable optimization technique, such as Golden Section search method [23], can be used to minimize (10) for a specific value of β, chosen by the user. A choice of β = 0.5 weighs both costs equally, whereas a choice of $\beta > 0.5$ emphasizes minimization of I_e over I_c, and $\beta < 0.5$ emphasizes minimization of I_c over I_e. Any specific choice of β yields a Pareto optimal solution [22]. Although the choice of β depends on the user's preference, it should not be chosen to be too close to either 0 or 1, because such extreme values emphasize one of the cost factors too heavily compared to the other.

An alternative way of choosing β is based on utilization of a min-max principle [24], which involves a two-step optimization process. The first step is basically same as what is described above, i.e., minimization of $f(\alpha, \beta)$ with respect to α for a particular choice of β. Suppose this yields an optimum value of the decision variable, α*, and the corresponding optimal function value,

$$f(\alpha^*, \beta) = \beta * [Ie(\alpha^*)] + (1 - \beta) * [Ic(\alpha^*)]. \quad (11)$$

Repetition of the above step for various values of β, yields a function, $f(\alpha^*, \beta)$, $0 \leq \beta \leq 1$. Next we need to choose an optimal value of β. To explain this choice, we follow the arguments given in [24]. Notice from Equation (10) that the main problem in choosing β is that if we choose it either too small (close to zero) or too large (close to 1), the right side of (10) effectively consists of only one of the cost components, minimization of which yields a very low value of $f(\alpha^*, \beta)$, which is suboptimal. Thus, one way to achieve a good trade-off between the two cost components in the right side of (10) is to seek a value of β that maximizes $f(\alpha^*, \beta)$. Thus, the second step of optimization involves finding $Max_\beta f(\alpha^*, \beta)$.

The above ideas are illustrated in Figures 2 and 3 below. For a typical value of β, $0 \leq \beta \leq 1$, Figure 2 illustrates the variation of the total cost, $f(\alpha, \beta)$, as a function of α. In this case, the optimal value of α turns out to be approximately 0.005. For a choice of β = 0.7, we get the optimal temperature profile shown in Figure 3.

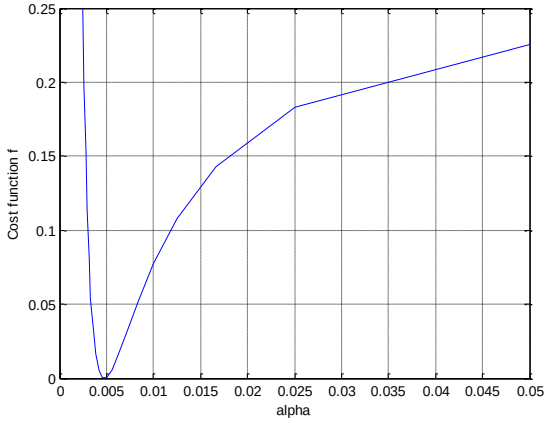

Figure 2. Total cost function $f^*(\alpha)$ vs α.

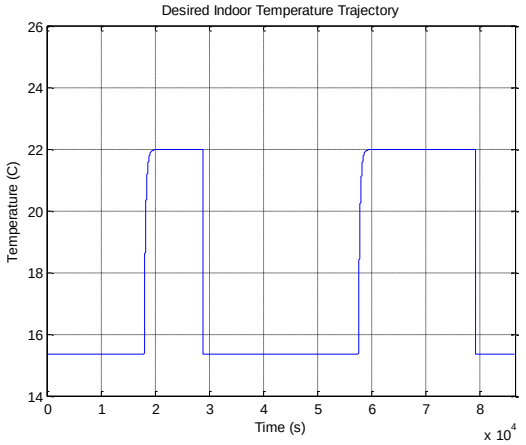

Figure 3. Optimal indoor temperature profile (for β = 0.7) between hours of 00:00 (12 am) and 23:59 (11:59 pm).

2.4. Application of an Optimum Reference Temperature Profile for Adaptive Control of Indoor Temperature

The design of adaptive OSA and WOSA controllers capable of following a reference temperature profile can be carried out in a straightforward way [11]. For the sake of brevity, only outlines are provided below, because this paper focuses mainly on optimization aspects and details of both OSA and WOSA can be found in [11,25].

2.4.1. Fixed One Step Ahead Control Algorithm

An OSA control law brings the current state $y(k+1)$ to the desired value $y^*(k+1)$ in one step. From Equation (4), it can be easily shown that the OSA control law is given by [11]:

$$\bar{u}(k) = \frac{y^*(k+1) - y(k) - T_s B[y_{out}(k) - y(k)] - T_s C}{[T_s A(y_{fav} - y(k))]}, \qquad kT_s \le t < (k+1)T_s \tag{12}$$

where T_s denotes the sampling interval. It is constrained by the maximum capacity of the furnace, u_{max}, as follows:

$$u(k) = \bar{u}(k) \quad \text{if } 0 < \bar{u}(k) < u_{max} \tag{13a}$$

$$\text{else} \quad u(k) = u_{max} \quad \text{if } \bar{u}(k) \ge u_{max} \tag{13b}$$

$$\text{else} \quad u(k) = 0 \quad \text{if } \bar{u}(k) \le 0 \tag{13c}$$

2.4.2. Fixed Weighted One Step Ahead Control Algorithm

In addition to output tracking, the goal of a WOSA control scheme is to regulate the control efforts by adding an extra term to the OSA cost function. The WOSA control law minimizes the following cost function:

$$J_2(k+1) = \frac{1}{2}[\hat{y}(k+1) - y^*(k+1)]^2 + \frac{\lambda}{2}u^2 \tag{14}$$

where $0 < \lambda < 1$ controls the trade-off between tracking and smoothness of control efforts. A larger value of λ reduces control efforts at the cost of higher tracking error and vice versa.

The control law minimizing the $J_2(k+1)$ is given by

$$\bar{u}(k) = \frac{[T_s A(y_{fav} - y(k))] * \{y^*(k+1) - y(k) - T_s B[y_{out}(k) - y(k)] - T_s C\}}{[T_s A(y_{fav} - y(k))]^2 + \lambda} \tag{15}$$

which is, once again, constrained by the maximum capacity of the furnace u_{max} as shown in Equations (13a–c).

2.4.3. Adaptive OSA and WOSA Temperature Controllers

In an adaptive controller, the sampled measurements, $u(k)$ and $y(k)$, are used to estimate the model parameters, A, B and C in Equation (2), using a recursive parameter estimation method, such as recursive least squares (RLS) [25]. The estimated values of theses parameters are then used to compute the OSA/WOSA control signals.

2.4.3.1. Parameter Estimation

First we write model Equation (2) in the following form:

$$y(k+1) = \varphi(k)^T \theta^* \tag{16}$$

where

$$\varphi(k) = [T_s * u(k-1)\{y_{fav} - y(k-1)\} \;\; T_s * \{y_{out}(k-1) - y(k-1)\} \;\; T_s]^T \tag{17a}$$

$$\theta^* = [A \;\; B \;\; C]^T \tag{17b}$$

2.4.3.2. Adaptive Control Algorithms

Next, the estimated value of θ^* is computed recursively using the recursive least squares (RLS) algorithm [11]. The adaptive OSA and WOSA controllers use the estimate, $\hat{\theta}(k)$, to compute the control signal, u(k), from the following adaptive versions of Equations (12) and (16):

For OSA: $$\bar{u}(k) = \frac{y^*(k+1) - y(k) - T_s\hat{B}(k)[y_{out}(k) - y(k)] - T_s\hat{C}\;(k)}{[T_s\hat{A}(k)\left(y_{fav} - y(k)\right)]} \tag{18}$$

For WOSA: $$\bar{u}(k) = \frac{[T_s\hat{A}(k)\left(y_{fav} - y(k)\right)] * \{y^*(k+1) - y(k) - T_s\hat{B}(k)[y_{out}(k) - y(k)] - T_s\hat{C}\;(k)\}}{[T_s\hat{A}(k)\left(y_{fav} - y(k)\right)]^2 + \lambda} \tag{19}$$

where $\hat{A}(k)$, $\hat{B}(k)$ and $\hat{C}(k)$ denote the estimated values of A, B and C, respectively, at time *k*.

2.4.4. Global Stability

Under mild assumptions, it can be shown that the above control law results in a globally stable system [11] and $\lim_{k\to\infty}|y(k) - y^*| = 0$.

3. Results and Discussion

In this section, we present the results of a simulation study of the proposed adaptive OSA and WOSA controllers by employing both arbitrary and optimal reference temperature profiles. This study focuses on a small single story residential home containing three bedrooms, one living room, a kitchen, and two bathrooms. The home is assumed to be rectangular in shape, with a living space of approximately 1200 square feet, and it is assumed to be heated by forced air delivered from a hydro-air heating system. The capacity of the heating unit is assumed to be 60,000 BTU, and it is assumed to have a continuously variable speed blower with a maximum discharge rate of 0.51 Kg/s, which is typical. Some of the physical and thermal characteristics of the building are listed in Table 1 below.

Table 1. Some physical and thermal characteristics of the building.

Total Volume of building	$V = 271\ m^3$	Overall Heat Transmittance	$H_T = 183\ W/K$
Specific Heat of air	$c_a = 1012\ J/Kg\ K$	Air Density	$\rho_a = 1.204\ Kg/m^3$
Average air temperature inside heat exchanger	$\theta_{fav} = 70$ ℃	Specific Heat of water	$c_f = 4186\ J/Kg\ K$
Thermal Gains	$Q_{gains} = Generated\ profile$		

For the purpose of this simulation, the average outdoor temperature during the cold months of winter in Midwest is assumed to vary sinusoidally between a low of −11 ℃ (12° F) to a high of 7.75 ℃ (46° F). This diurnal variation of temperature is approximated by the following equation:

$$y_{out}(t) = -1.67 - 9.4cos(\frac{2\pi t}{24*3600}). \quad (21)$$

Also, the diurnal heat gains from solar and other sources, such as lighting, appliances and occupants, are assumed to follow the profiles depicted in Figures 4 and 5, respectively.

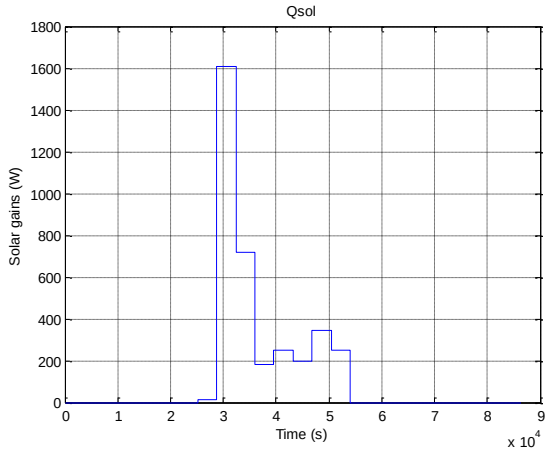

Figure 4. Profile of diurnal solar heat gains.

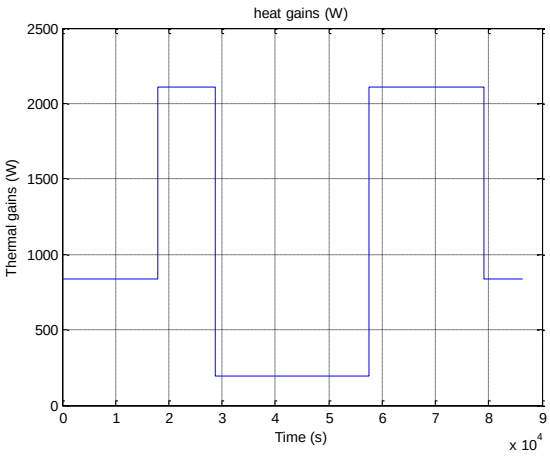

Figure 5. Profile of diurnal heat gains from lighting, appliances and occupants.

To start with, we discuss the results of simulation of adaptive OSA and WOSA controllers for an arbitrarily chosen steep-ascent reference temperature profile, as shown in Figure 1a. As mentioned earlier, such a steeply ascending temperature profile emphasizes comfort over cost, which is likely to increase the consumption of heat energy.

For the adaptive OSA controller, the variation of indoor temperature and the control efforts are shown in Figures 6a and 6b, respectively. Figure 6a shows excellent tracking between the indoor temperature and the reference temperature, which is expected from a typical OSA controller. The corresponding control efforts, shown in Figure 6b, is seen to be somewhat bumpy, which is also expected from an OSA controller. The adaptive WOSA controller, on the other hand, attempts to seek a trade-off between tracking error and control efforts by minimizing the cost function given by Equation (15), where λ controls the trade-off between tracking error and control efforts. The performance of adaptive WOSA for a choice of $\lambda = 0.1$ is shown in Figures 7a and 7b. As expected, a comparison of Figures 6a and 7a shows that the WOSA controller exhibits moderate tracking errors, but on the positive side, it smooths the control efforts, which can be seen by comparing Figures 6b and 7b.

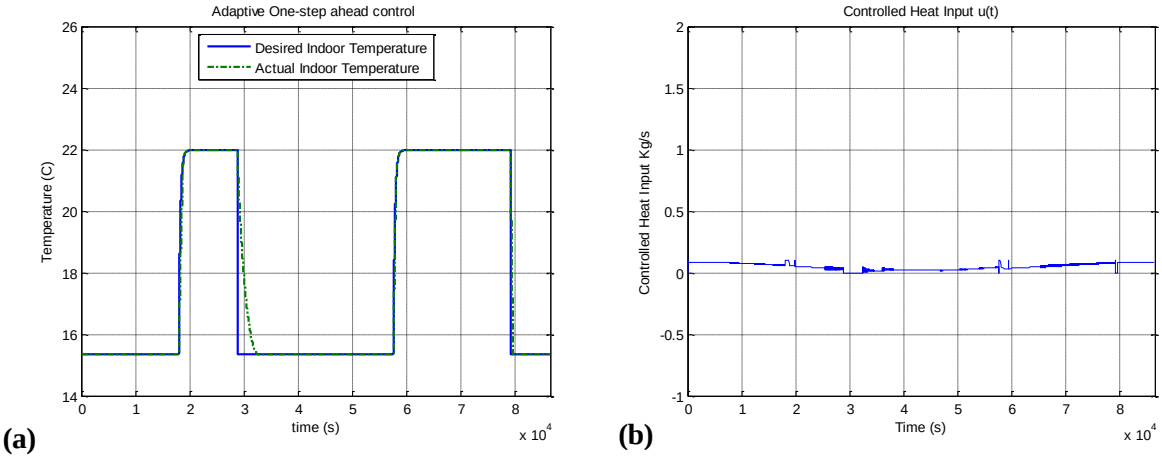

Figure 6. Performance of adaptive OSA controller for an arbitrarily chosen steep-ascent reference temperature profile: (a) Indoor temperature, y(t), (b) Air flow rate, u(t).

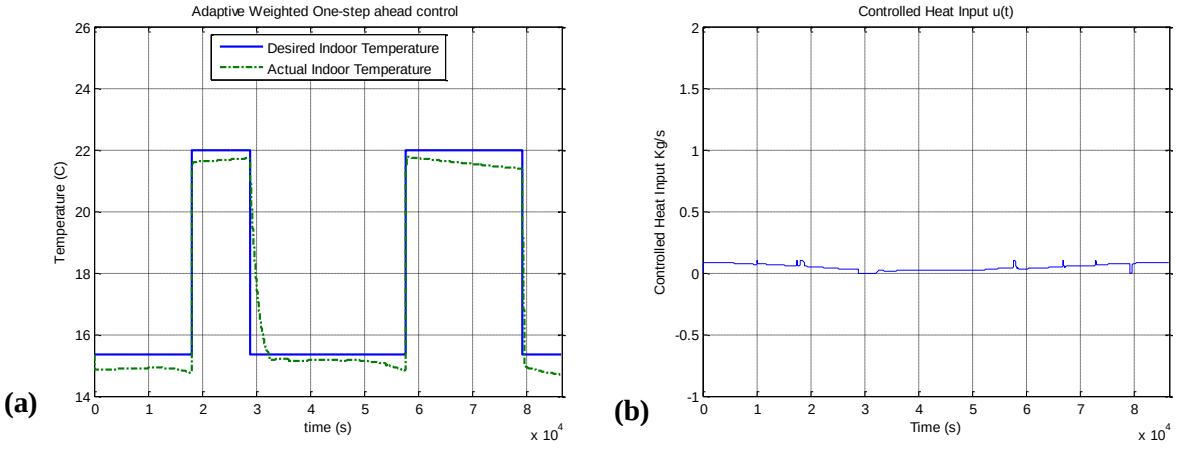

Figure 7. Performance of adaptive WOSA controller for an arbitrarily chosen steep-ascent reference temperature profile: (a) Indoor temperature, y(t), (b) Air flow rate, u(t).

Next, we discuss the simulation results for an optimal reference temperature profile, shown in Figure 3. As mentioned earlier, such an optimal temperature profile attempts to seek a trade-off between the costs of discomfort and energy, by choosing an appropriate value of β in the total cost function described by Equation (10). In this study, we chose $\beta = 0.7$, which weighs the cost of energy slightly more than the cost of discomfort. The tracking error and control efforts for the adaptive OSA controller are depicted in Figures 8a and 8b, whereas the same for the adaptive WOSA controller are shown in Figures 9a and 9b, respectively. These exhibit essentially similar characteristics, as discussed above.

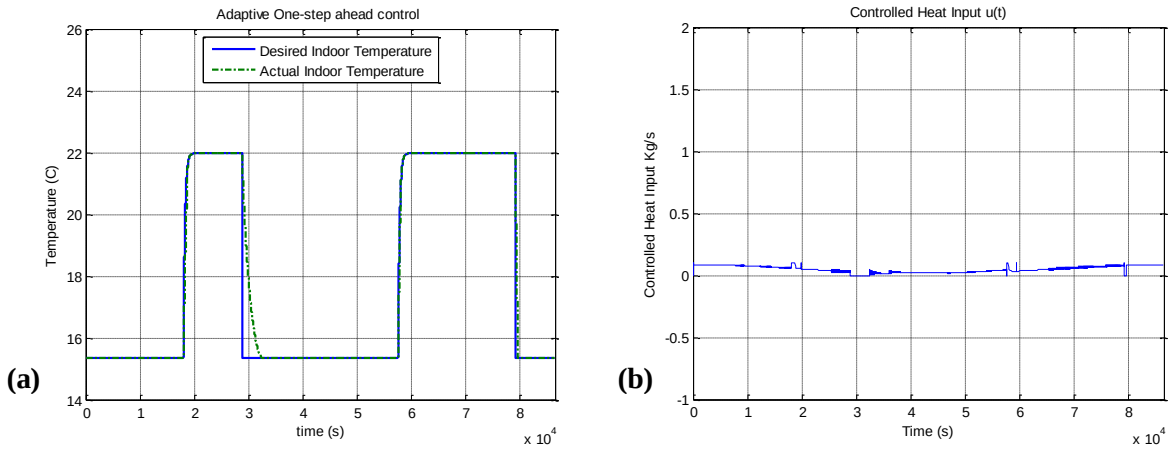

Figure 8. Performance of adaptive OSA controller using an optimal reference temperature profile (for $\beta = 0.7$): (a) Indoor temperature, y(t); (b) Air flow rate, u(t).

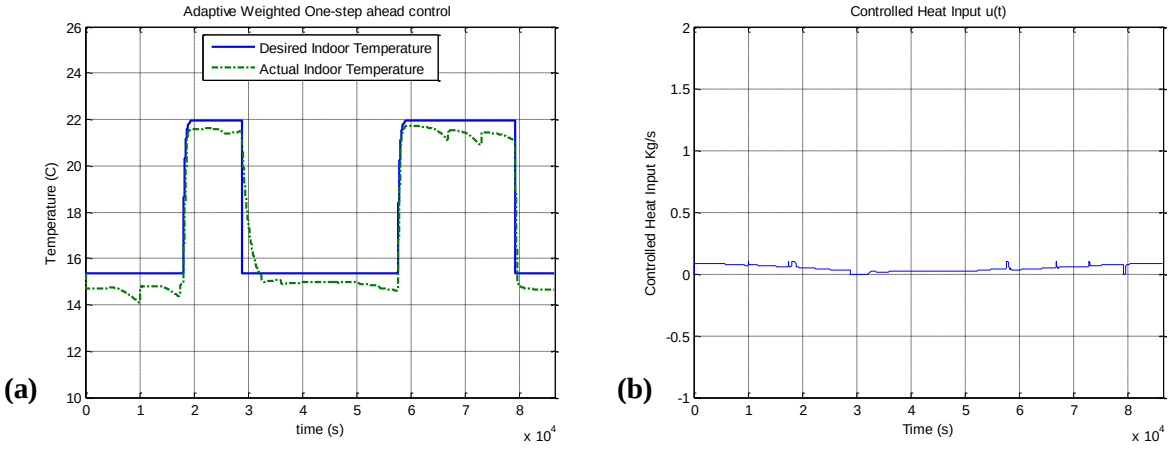

Figure 9. Performance of adaptive WOSA controller for an optimal reference temperature profile (for $\beta = 0.7$): (a) Indoor temperature, y(t), (b) Air flow rate, u(t).

Finally, the potential for daily energy savings depends on various factors, such as outdoor temperature, maximum heat delivery capacity of the furnace, number of up-down temperature cycles, etc. Our preliminary simulation results indicate that both OSA and WOSA controllers can reduce daily heating energy consumption by more than 5%, as compared to the energy consumed by using an arbitrarily chosen steep-ascent temperature profile. This just illustrates the feasibility of the proposed optimization concept. In fact, such energy savings can be increased significantly by

choosing more efficient temperature profiles characterized by three or more temperature settings and more frequent hops between them. Also, considering the accumulated savings over an entire cold season lasting four to five months, the resulting savings can be significant. An additional benefit of OSA and WOSA controllers may result from the savings in capital and maintenance costs of the furnace, because such controllers can meet the heating needs of a building by using furnaces of significantly lower capacity. These and other related cost saving aspects are currently under investigation.

4. Conclusion

This paper presents a technique for designing optimum reference temperature profiles for energy-efficient control of indoor temperature in buildings. With the dual goal of energy efficiency and occupants' comfort in mind, we formulate a multi-objective cost function that consists of a weighted sum of both costs, with individual weights being chosen by the user. This cost function is then minimized to generate an optimum reference temperature profile. Finally, the usage of such a temperature profile for controlling indoor temperature is demonstrated by designing a one-step ahead adaptive temperature controller for a single story residential building. A comparative evaluation of the performance of the proposed controller with and without the optimized temperature profile shows that the controller with the optimization temperature profile performs better and also saves energy.

Conflict of interest

All authors declare no conflicts of interest in this paper.

References

1. Paris B, Eynard J, Grieu S, et al. (2010) Heating control schemes for energy management in buildings. *Energ Buildings* 42: 1908-1917.
2. Dounis A, Caraiscos C (2009) Advanced control systems engineering for energy and comfort management in a building environment-A review. *Renew Sust Energ Rev* 13: 1246-1261.
3. Moon J, Jung S, Kim Y, et al. (2011) Comparative study of artificial intelligence based building thermal control methods-application of fuzzy, adaptive neuro-fuzzy inference system, and artificial neural network. *Appl Therm Eng* 31: 2422-2429.
4. Afram A, Sarifi F (2014) Theory and Applications of HVAC Control Systems – A Review of Model Predictive Control. *Build Environ* 72: 343-355.
5. Hazyuk I, Ghiaus C (2014) Model predictive Control of thermal comfort as a benchmark for controller performance. *Automat Constr* 43: 98-109.
6. Privara, S, Siroky J, Ferkl L, et al. (2011) Model Predictive Control of a building heating system: The first experience. *Energ Buildings* 43: 564-572.
7. Balan R, Cooper J, Chao K, et al. (2011) Parameter identification and model based predictive control of temperature inside a house. *Energ Build* 43: 748-758.
8. Ma Y, Borrelli F, Hencey B, et al. (2011) Haves P. Model predictive control for the operation of building cooling systems. *IEEE Trans Contr Syst Technol* 99: 1-8.

9. Calvino F, Gennusa M, Morale M, et al. (2010) Comparing different control strategies for Indoor thermal comfort aimed at the evaluation of the energy cost of quality of building. *Appl Therm Eng* 30: 2386-2395.
10. Orosa J (2011) A new modeling methodology to control HVAC systems. *Expert Syst Appl* 38: 4505-4513.
11. Chaudhry S, Das M (2014) A Stable Adaptive Control Scheme for Building Heating and Cooling Systems. *J Power Energy Eng* 2: 14-25.
12. Hongli1 L, Peiyong D, Qingmei Y, et al. (2012) A Novel Adaptive Energy-efficient Controller For the HVAC Systems. *Proceedings of 24th CCDC*, 1402-1406.
13. Perrera D, Pfeiffer C, Skeie N (2014) Control of temperature and energy consumption in buildings—A review. *Int J Energy Environ* 5: 471-484.
14. Wang S, Gao D, Sun Y, et al. (2013) An online adaptive optimal control strategy for complex building chilled water systems involving intermediate heat exchangers. *Appl Therm Eng* 50: 614-628.
15. Lu L, Cai W, Chai Y, et al. (2005) Global optimization for overall HVAC systems—Part I problem formulation and analysis. *Energ Convers Manage* 46: 999-1014.
16. Lu L, Cai W, Chai Y, et al. (2005) Global optimization for overall HVAC systems—Part II problem solution and simulations. *Energ Convers Manage* 46: 1015- 1028.
17. Kusiak A, Li M, Tang F (2010) Modeling and optimization of HVAC energy consumption. *Appl Energy* 87: 3092-3102.
18. Ghiaus C (2013) Causality issue in the heat balance method for calculating the design heating and cooling load. *Energy* 50: 292-301.
19. IBPT International Building Physics Toolbox in Simulink. Available from: http://www.ibpt.org
20. Fanger P (1972) Thermal Comfort: Analysis and Applications in Environmental Engineering, New York: McGraw-Hill.
21. Ashrae ANSI, Thermal Environmental Conditions for Human Occupancy. American Society of Heating, Refrigerating and Air-Conditioning Engineers, Atlanta, GA, 2004
22. Marler R, Arora J (2004) Survey of multi-objective optimization methods for engineering. *Struct Multidiscip O* 26: 369-395.
23. Rao S (2009) Engineering Optimization: Theory and Practice, 4th ed., New Jersey: John Wiley and Sons.
24. Gennert M, Yuille A (1988) Determining The Optimal Weights In Multiple Objective Function Optimization. *Proceedings of Second International Conference on Computer Vision*, 87-89.
25. Goodwin G, Sin K (1984) Adaptive filtering prediction and control, New Jersey: Prentice-Hall.

AIMS Press